Binding of Phlorizin to the Isolated C-Terminal Extramembranous Loop of the Na^+/Glucose Cotransporter Assessed by Intrinsic Tryptophan Fluorescence

Xiaobing Xia, Jiann-Tso Lin, and Rolf K. H. Kinne*

Department of Epithelial Cell Physiology, Max Planck Institute for Molecular Physiology, Otto-Hahn-Strasse 11, 44227 Dortmund, Germany

Received December 10, 2002; Revised Manuscript Received March 4, 2003

ABSTRACT: Phlorizin, a phloretin 2′-glucoside, is a potent inhibitor of the Na^+/glucose cotransporter (SGLT1). On the basis of transport studies in intact cells, a binding site for phlorizin was suggested in the region between amino acids 604−610 of the C-terminal loop 13. To further investigate phlorizin binding titration experiments of the intrinsic Trp fluorescence of isolated wild-type loop 13 and two mutated loops (Y604K and G609K) were carried out. Phlorizin (135 μM) produced approximately 40% quenching of the fluorescence of wild-type loop 13; quenching could also be observed with the two mutated loops. The apparent K_d was lowest for the wild-type loop 13 ($K_d \approx 23$ μM), followed by mutant G609K (57 μM) and mutant Y604K (70 μM). Binding of phlorizin was further confirmed by a decrease of the accessibility of loop 13 to the collisional quencher acrylamide. The interaction involves the aromatic moiety of the aglucone since phloretin (the aglucone of phlorizin) showed almost the same effects as phlorizin, while D-glucose did not. MALDI-TOF experiments revealed that loop 13 contained a disulfide bond between Cys 560 and Cys 608 that is very important for phlorizin-dependent fluorescence quenching. These studies provide direct evidence that loop 13 is a site (important amino acids including 604−609) for the molecular interaction between SGLT1 and phlorizin. They confirm that the aglucone part of the glucoside is responsible for this interaction.

SGLT1,[1] a member of the Na^+-dependent glucose cotransporter family, is localized in the apical plasma membrane of epithelial cells in the small intestine and the kidney, where it is responsible for absorption or reabsorption of sugars. SGLT1 mediates secondary active, high-affinity transport of glucose driven by the Na^+ gradient across the membrane. Owing to its key physiological role in maintaining glucose homeostasis, SGLT1 has been extensively characterized with respect to its transport mechanism. Conformational changes in rabbit SGLT1 could be found in the presence of Na^+, which increases the cotransporter's affinity for sugar (*1*, *2*). Similarly, by monitoring the intrinsic fluorescence of the protein, a galactose/glucose-dependent conformation change could be observed in a bacterial Na^+-dependent galactose/glucose cotransporter of the SGLT family (*3*). Extensive mutagenesis studies showed that Na^+ binding sites are at the N-terminal half of the protein, while glucose binds and permeates through the C-terminal half of the cotransporter (*4*, *5*). It was further suggested that amino acids 162−173 constitute part of an external Na^+ pore in the SGLT1 protein, while the residues Gln 457 and Thr 460 control the sugar binding (*6*, *7*). Phlorizin, a β-glucoside of the aromatic compound phloretin, is the most potent competitive D-glucose transport inhibitor among the known glucosides, with a K_i value of 1 μM (*8*). It is proposed that the phlorizin binding to the SGLT1 from rabbit renal brush border membrane vesicles is a two-step process: rapid formation of an initial collision complex followed by a slow isomerization process that occludes phlorizin within its receptor site (*9*). Phlorizin is thereby supposed to bind to both the sugar binding site and the aglucone binding site, the latter with a hydrophobic/aromatic surface (*10*, *11*).

In our laboratory, we have performed a series of site-directed mutagenesis studies to search for the phlorizin binding region. Our recent results indicated that the hydrophobic region located in the C-terminal loop 13 (amino acids 604−610) is critically involved in the binding of phlorizin (*12*).

To further characterize the structure−function relationship of loop 13, we took advantage of advances in gene expression and application of biophysical methods to investigate the phlorizin binding region in vitro. The wild type loop 13 and two mutants with supposedly lower affinity to phlorizin were expressed in *Escherichia coli*, purified, and refolded in vitro. The single Trp residue in the peptide enabled us to study the interaction of loop 13 with the substrates. Quenching of Trp fluorescence and the different accessibility of the Trp residue to acrylamide in the presence or absence of phlorizin were thereby used as signals.

* Correspondence to Rolf K. H. Kinne; e-mail: rolf.kinne@mpi-dortmund.mpg.de; phone: +49 (0) 231 − 133 2200; fax: +49 (0) 231 − 133 2299.

[1] Abbreviations: SGLT1, Na^+/glucose cotransporter; GnHCl, guanidine hydrochloride; IPTG, isopropyl-β-D-thiogalactopyranoside; GSH, reduced glutathione; GSSG, oxidized glutathione; 2-ME, β-mercaptoethanol; PCR, polymerase chain reaction; SDS−PAGE, sodium dodecyl sulfate−polyacrylamide gel electrophoresis; FRET, fluorescence resonance energy transfer; K_d, equilibrium dissociation constant; K_{sv}, collisional quenching constant; MALDI, matrix-assisted laser desorption ionization; TOF, time-of-flight.

10.1021/bi020695b CCC: $25.00
Published on Web 04/26/2003

The studies reported below clearly indicate that loop 13 can bind phlorizin also in an isolated form and support the notion that the region between amino acids 604−609 contributes to this interaction mainly by providing a binding site for the aromatic aglucone moiety of the glucoside.

EXPERIMENTAL PROCEDURES

Chemicals and Enzymes. Restriction enzymes, T4 DNA ligase, Taq DNA polymerase, and dNTP were obtained from Promega (Mannheim, Germany) or New England Biolabs (Schwalbach, Germany). Oligonucleotides were synthesized by MWG Biotech (Ebersberg, Germany). The pET-28a plasmid and BL21 (DE3) cells were from Novagen (Madison, WI). Ni^{2+}-NTA agarose was purchased from Qiagen (Karlsruhe, Germany). Dialysis membrane was obtained from Spectrum Laboratory Inc. (Rancho Dominguez, CA). Sucrose was purchased from Serva (Heidelberg, Germany). The following chemical reagents were from Sigma (Taufkirchen, Germany), Gerbu Biotechnik (Gailberg, Germany) or Roth (Karlsruhe, Germany): EDTA, Tris-base, glycine, NaCl, phlorizin, phloretin, D-glucose, guanidine hydrochloride, isopropyl-β-D-thiogalactopyranoside, urea, reduced and oxidized glutathione, β-mercaptoethanol, L-tryptophan, in the highest purity available.

Expression and Purification of the Wild-Type and Mutated Loop 13. cDNAs coding for the wild-type loop 13 (amino acids 549−638) and the two mutated loops (G609K and Y606K) were amplified by PCR using the plasmid templates described before (*12*). PCR products with the correct sequences were introduced into pET-28a, in which the poly-His sequences were placed at both the N- and C-terminus of loop 13. BL21 (DE3) cells containing the recombinant plasmid were grown in 2 × TY medium and induced with 0.5 mM IPTG. The His-tagged proteins, which were expressed as inclusion bodies, were solublized with a Na_2HPO_4 buffer (100 mM Na_2HPO_4, 200 mM NaCl, 10 mM imidazole, 10% sucrose) at pH 8.0 containing 8 M GnHCl and then passed through a Ni^{2+}-NTA affinity column charged with 10 mM $NiSO_4$. After extensive washing of the sample with Na_2HPO_4 buffer at pH 6.4 containing 6 M GnHCl, loop 13 possessing the poly-His tags was eluted from the column with Na_2HPO_4 buffer at pH 4.5 containing 6 M GnHCl. Proteins were refolded through exhaustive dialysis against refolding buffer A (3 M urea, 50 mM Tris-HCl, 1 mM GSH, 0.1 mM GSSH, pH 7.2) and refolding buffer B (50 mM Tris-HCl, 50 mM glycine, 100 mM NaCl, 10% sucrose, 0.1 mM GSH, 0.01 mM GSSH, 1 mM EDTA, adjusted to pH 7.2), respectively. To increase the purity, the refolded proteins were further purified through a Mono Q HR column (Amersham Biosciences, Freiburg, Germany). The proteins used for biophysical analysis were checked by SDS−PAGE and the purity was estimated to about 90% (Figure 1B). Protein concentration was determined by the Bradford method.

Sulfhydryl Modification. The states of the two cysteine residues of loop 13 were determined by specific labeling of the free SH group. To get the reduced wild-type loop 13 for labeling, protein (about 10 μM) was incubated with 25 mM 2-ME at room temperature for 1 h, and excess 2-ME was removed from the reduced protein by desalting through a HiTrap desalting column (Amersham Biosciences, Freiburg, Germany). Biotinylation of the cysteine residues of the loop

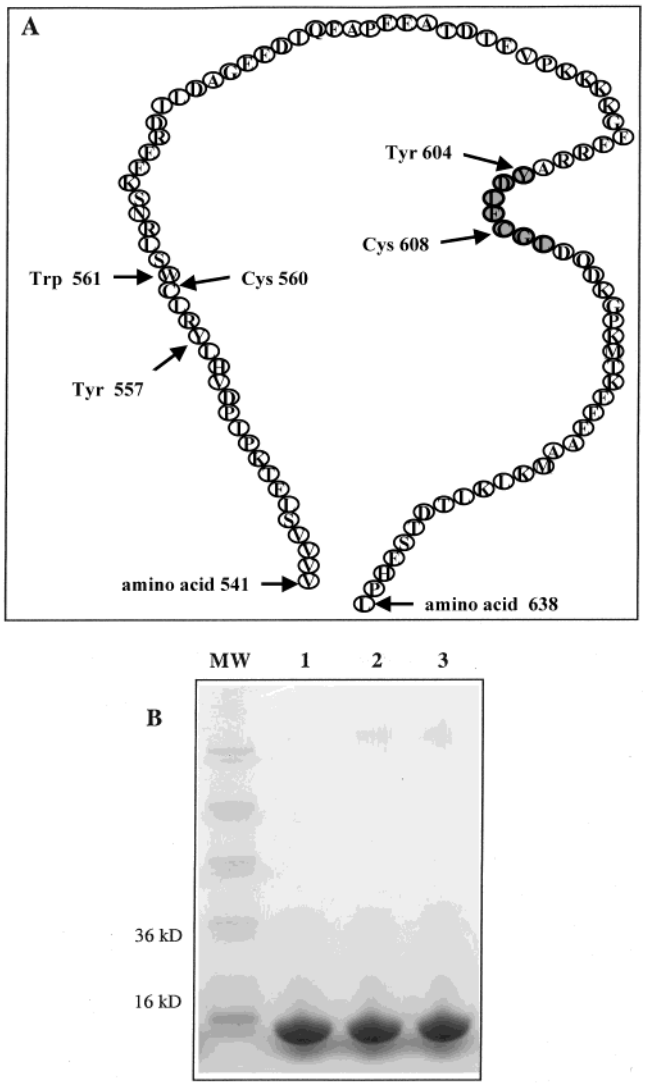

FIGURE 1: (A) The primary sequence of loop 13 of rabbit SGLT1 (amino acids 541−638). The presumed phlorizin binding region is shown in gray. The position of Trp, Tyr, and Cys are indicated. (B) SDS−PAGE gel following the anion exchange chromatography purification of His-tagged loop 13. About 20 μg of protein was loaded on each lane. SDS−PAGE was performed using a precast Bis-Tris 4−12% gel (Invitrogen, CA) in Tris-glycine running buffer. Lane 1: protein molecular weight standard, lane 2: mutant G609K, lane 3: mutant Y604K, lane 4: wild-type loop 13.

13 and reduced loop 13 with (+)-biotinyl-iodoacetamidyl-3,6-dioxaoctanediamine (PEO−iodoacetyl−biotin) (Perbio Science, Bonn, Germany) was carried out in the dark for 60 min at room temperature. Protein was then precipitated with trichloroacetic acid and solublized with 40% acetic acid for MALDI-TOF mass spectrometry analysis.

MALDI-TOF Mass Spectrometry. Mass spectra were acquired in the positive ion, linear mode on a Voyager DE-PRO MALDI (PE-Biosystems, Shelton, USA). After mixing the solubilized protein with matrix (saturated sinapinic acid from Sigma in 50% acetonitrile with 0.1% trifluoroacetic acid), samples were loaded on a MALDI plate and dried at room temperature.

Fluorescence Spectroscopy. Steady-state fluorescence studies were carried out at room temperature in a Perkin-Elmer LS 50B spectroscope (Perkin-Elmer, USA), fitted with a 450-W xenon arc lamp, using 5-nm slits for both excitation and emission. A 0.3-cm excitation and emission path length

quartz cell was used for all the fluorescence measurements. Emission spectra were taken from 300 to 400 nm with a fixed excitation wavelength of 280 or 295 nm, averaging three scans. Excitation spectra were taken from 250 to 300 nm in 5-nm bandwidths at a fixed emission wavelength of 350 nm, averaging three scans.

Ligand-Dependent Fluorescence Quenching. The binding of substrates to loop 13 was monitored by ligand-induced fluorescence quenching as a function of the concentration of phlorizin or phloretin. After the substrates were incubated with proteins at room temperature for 2 min, fluorescence was recorded at an excitation wavelength of 295 nm and emission wavelength of 340 nm. Measurements were performed at a concentration range of 1−135 μM phlorizin or phloretin in a total volume of 300 μL. In all cases, the protein concentrations were 3.0 μM in 50 mM Tris-HCl, 100 mM NaCl, 1 mM EDTA, pH 7.2. The inner filter effect of substrates which is due to their absorbance at the excitation and the emission wavelengths range of Trp was subtracted using the following equation (*13*):

$$F_{corr} = F_{obs}\ \text{antilog}[(A_{ex} + A_{em})/2] \quad (1)$$

where A_{ex} and A_{em} were the absorbance of the substrates at 295 nm and emission at 340 nm, respectively, F_{corr} and F_{obs} were the corrected and observed fluorescence intensity. To check whether eq 1 works well in our case, titration of L-Trp (3 μM) with the substrates (excitation at 295 nm; emission at 355 nm) was also performed to obtain the correction factor ($C_{ex} = F_{corr}/F_{obs}$). In the range of substrate concentrations used (less than 135 μM), the difference between the C_{ex} obtained through the equation and Trp titration is very small; therefore, we used the eq 1 to correct for the inner filter effects of the substrates. At least three experiments were performed at each data point. The corrected relative fluorescence intensity at different substrate concentrations was determined and was fitted to a single-site binding equation using a nonlinear least-squares fit program. The binding constants for phlorizin were obtained using a nonlinear analysis program, Prism (Graphpad, San Diego, USA).

Stern−Volmer Quenching. Up to 350 mM acrylamide was added from a 5 M solution to 3 μM protein in 50 mM Tris-HCl buffer containing 100 mM NaCl, 1 mM EDTA, pH 7.2 either in the absence or in the presence of 30 μM phlorizin at room temperature at a final sample volume of 300 μL. After each addition the solution was mixed and after 5 min the Trp fluorescence spectra were measured using an excitation at 295 nm and an emission at 340 nm. The data were analyzed according to the Stern−Volmer equation (*13*):

$$F_0/F = 1 + K_{sv}[Q] \quad (2)$$

where F_0 is the fluorescence of protein in the absence of acrylamide, F is the observed fluorescence, [Q] is the acrylamide concentration, and K_{sv} is the collisional quenching constant. 3 μM L-Trp solution was used as a Stern−Volmer quenching control (excitation at 295 nm with fluorescence emission at 355 nm).

RESULTS

Quenching of Intrinsic Fluorescence and Phlorizin Binding. In the presence of 1−135 μM phlorizin, the fluorescence of the wild-type loop 13 and the two mutated loops was studied with excitation at 295 nm and emission at 340 nm. Significant fluorescence quenching for wild type and mutated loops could be observed in the presence of high concentrations of phlorizin. The titration of wild-type loop 13 and the two mutants with different concentration of phlorizin is shown in Figure 2. About 40% of the intrinsic fluorescence of wild-type loop 13 was quenched in a dose-dependent manner. The estimated equilibrium dissociation constant (K_d) of the wild-type loop 13 is around 23 μM. With identical concentrations of G609K and Y604K, the quenching of the intrinsic fluorescence was significantly smaller, and the saturation point could not be reached. Assuming that at saturation, all three proteins exhibit the same degree of intrinsic fluorescence quenching by phlorizin, an apparent K_d value of 57 μM for G609K and of 70 μM for Y604K could be calculated (see Table 1).

Acrylamide Quenching. Titration with the water-soluble collisional quencher was also used to measure accessibility

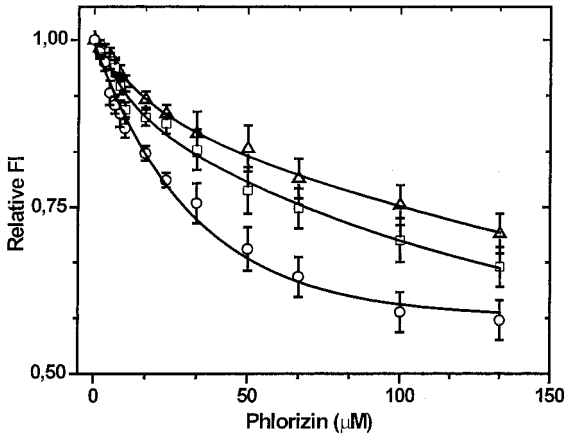

FIGURE 2: Quenching of the intrinsic protein fluorescence by phlorizin. Titration was performed as described in Experimental Procedures. Samples included wild-type loop 13 (○), G609K (□), and Y604K (△). Fluorescence measurements were performed at an excitation wavelength of 295 and an emission wavelength of 340 nm. The fluorescence intensity (FI) at 340 nm was corrected for the inner filter effects and used to calculate the relative FI (F/F_0, where F is the FI in the presence of phlorizin and F_0 is the FI in absence of phlorizin). The percentage of quenching at saturating phlorizin concentration for wild-type loop 13 was calculated from the data and an equilibrium dissociation constant (K_d) was determined using Prism (Graphpad, San Diego, CA). The K_d values of the Y604K and G609K were determined by assuming that the percentages of quenching were the same as that of wild-type loop 13 at saturating phlorizin concentrations. The K_d values obtained are summarized in Table 1. Mean values ± SD of at least three independent experiments are given.

Table 1: Phlorizin Binding to the Wild Type and Mutated Loop 13

protein	apparent K_d[a] (μM)	apparent K_i of phlorizin[b] (μM)
wild type	23 ± 2	4.6
G609K	57 ± 7	60.2
Y604K	70 ± 10	75.3

[a] The apparent equilibration dissociation constant (K_d) were determined from nonlinear regression analysis of the percentage of fluorescence quenching (Figure 2) as a function of phlorizin concentration using a computer based analysis program (Prism). To determine the K_d of the mutants, we assumed that their percentage of fluorescence quenching is the same as that of wild type at the saturating phlorizin concentration. Values are the mean ± SD. [b] Apparent K_i values of phlorizin action on α-methyl D-glucose uptake into transfected cells are from Novakova et al. 2001 (*12*).

Table 2: Accessibility of Trp 561 in Wild Type Loop 13 and Mutants to Acrylamide Fluorescence

protein	phlorizin[a]	K_{sv}[b] (M^{-1})	SD
L-Trp	−	22.09	1.15
	+	22.14	1.15
wild-type loop 13	−	2.84	0.13
	+	1.84	0.08
mutant G609K	−	2.18	0.14
	+	1.98	0.14
mutant Y604K	−	2.33	0.08
	+	2.22	0.12

[a] Quenching experiments were performed in the presence (+) or absence (−) of 30 μM phlorizin (Figure 3). [b] The Stern−Volmer quenching constants were obtained from the slopes of the linear regression lines for plots of $F_0/F = 1 + K_{sv}[Q]$. Values are mean ± SD.

of loop 13 Trp to acrylamide upon phlorizin binding. Stern−Volmer plots for acrylamide quenching of the wild-type loop 13 and the two mutated loops in the absence and presence of phlorizin are shown in Figure 3. The quenching profiles were linear with coefficients higher than 0.99. The Stern−Volmer constants for the three proteins are compiled in Table 2. Upon phlorizin binding, the Stern−Volmer constant decreased for the wild-type loop 13, indicating a protection effect by phlorizin. At 30 μM phlorizin, slight protection effects were also observed with G609K and almost no protection for Y604K. Thus, again, the affinity of the wild-type loop 13 to phlorizin appears to be the highest and the affinity of Y604K the lowest. The protection effect was not observed with L-Trp solution (3 μM) in the presence of 30 μM phlorizin.

Titration of Fluorescence of Loop 13 with Phloretin and D-Glucose. Phloretin, the aglucone of phlorizin, was also used to titrate the Trp fluorescence of wild-type loop 13. As can be seen from Figure 4, phloretin elicited almost the same quenching as phlorizin. From the concentration dependence of quenching an apparent equilibrium dissociation constant of 25 μM could be derived. To investigate whether the sugar moiety of the glucoside phlorizin also induced fluorescence changes, D-glucose was used for titration. No fluorescence changes could be observed even in the presence of 10 mM glucose.

A Disulfide bond between Cys 560 and Cys 608 is Important for Fluorescence Quenching. Loop 13 contains two cysteine residues (Cys 560 and Cys 608), one located adjacent to Trp561 and another located in the region that is important for phlorizin binding (Figure 1A). Figure 5 shows that after treatment with 25 mM 2-mercaptoethanol, both of the two cysteine residues of loop 13 were modified by PEO−iodoacetyl−biotin while no modification occurred without treatment with 2-ME. Since PEO−iodoacetyl−biotin is a sulfhydryl-reactive biotinylation reagent, it can be concluded that the two cysteine residues normally form a disulfide bond. We also observed that at 100 μM phlorizin, the decrease of tryptophan fluorescence intensity was less than 5% in the presence of excess 2-ME, while without 2-ME, the intrinsic fluorescence intensity quenching was around 40%.

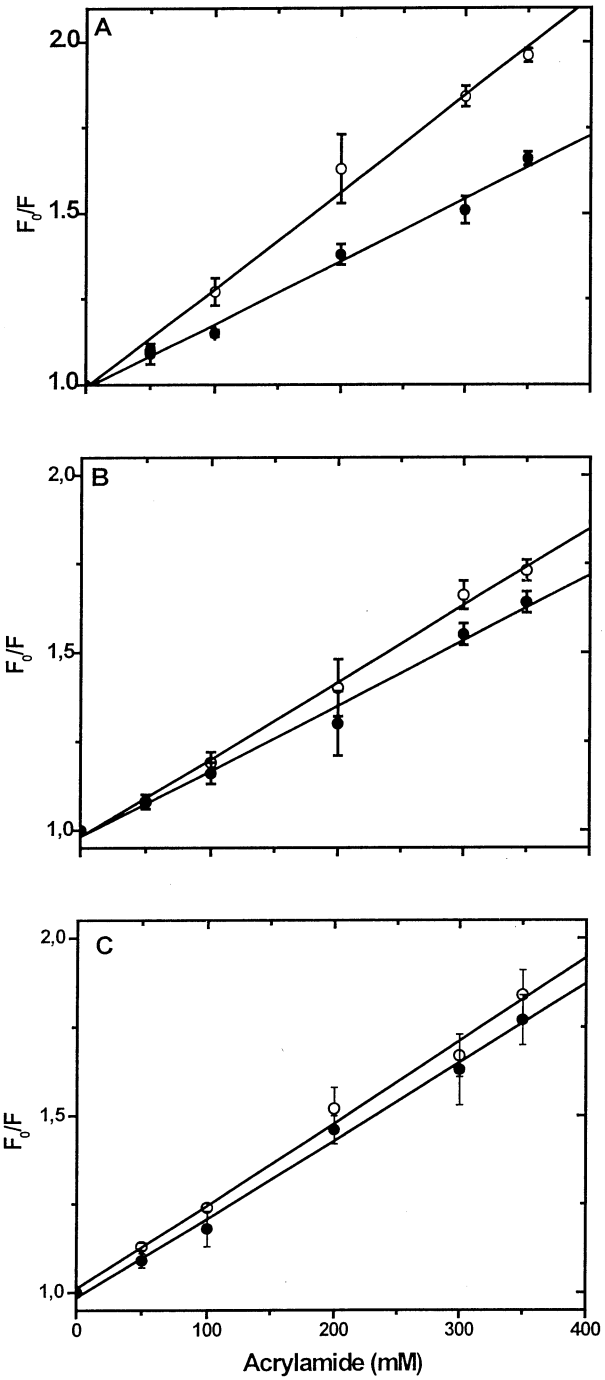

FIGURE 3: Stern−Volmer plots of the acrylamide quench of the steady-state fluorescence of the proteins. Quenching experiments were conducted as described under Experimental Procedures. Fluorescence measurements were performed at an excitation wavelength of 295 nm and an emission wavelength of 340 nm. In each panel, the samples were investigated in the presence (●) or absence (○) of 30 μM phlorizin. The protein samples include wild-type loop 13 (A), mutant G609K (B), and mutant Y604K (C). F_0 is the fluorescence intensity in the absence of acrylamide and F is the fluorescence intensity in the presence of acrylamide. The slopes (K_{sv}) of the best fit lines for each protein are shown in Table 2. Mean values ± SD of three independent experiments are given.

DISCUSSION

We have successfully overexpressed the loop 13 of SGLT1 in *E. coli*. By optimizing the purification and refolding protocol, the wild type and the two mutated loop proteins could be obtained in sufficient purity for biophysical analysis of the structure−function relationship of loop 13. Phlorizin binding to the loop could be demonstrated by phlorizin-dependent fluorescence quenching and by protection of the acrylamide-dependent fluorescence quenching by phlorizin. We thereby demonstrated that an isolated loop 13 also can

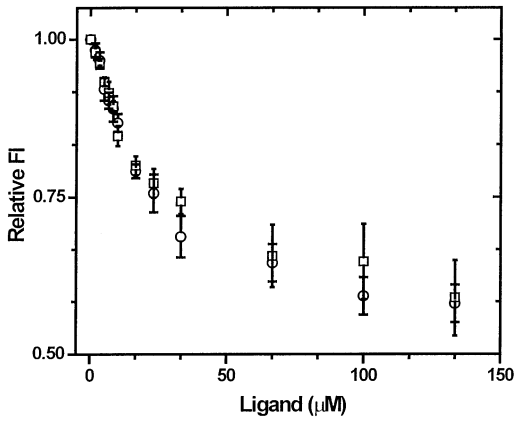

FIGURE 4: Quenching of the intrinsic protein fluorescence upon phlorizin or phloretin addition. Fluorescence measurements were performed at an excitation wavelength of 295 nm and an emission wavelength of 340 nm. The observed fluorescence intensities were corrected for the inner filter effects. Titration of the fluorescence of wild-type loop 13 with either phlorizin (○) or phloretin (□) was performed. Mean values ± SD of three independent experiments are given.

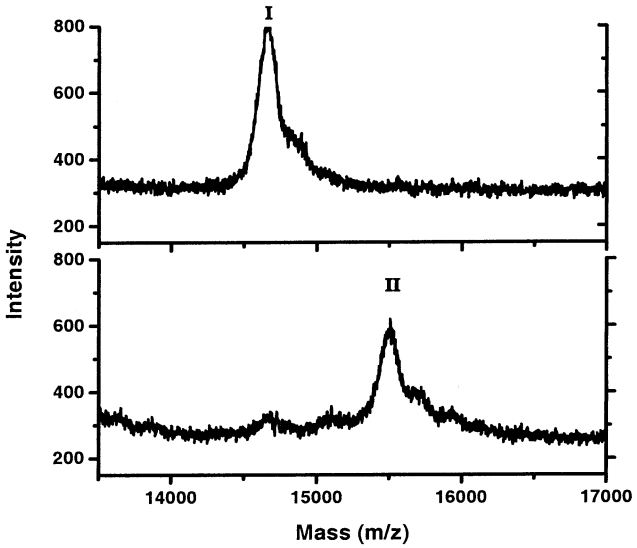

FIGURE 5: Mass spectroscopy of the wild-type loop 13 labeled with PEO−iodoacetyl−biotin. MALDI-TOF mass spectroscopy was used to analyze the state of the two cysteine residues. After incubation of loop 13 with PEO−iodoacetyl−biotin (MW 542 Da) directly, a mass of 14554 Da (peak I) which is very close to the theoretical average mass of loop 13 was observed. After incubation with 2-ME and subsequent labeling with PEO−iodoacetyl−biotin, a protein mass of 15384 Da (peak II) could be found. The labeling reactions were performed at a pH of 8.3. Since PEO−iodoacetyl−biotin specifically modifies free SH groups, an increase of molecular weight of about 415 Da per SH group can be expected. The difference found is 830 Da, suggesting that the two cysteine residues in loop 13 form a disulfide bridge.

interact with phlorizin as postulated for the loop 13 in the complete and intact rabbit SGLT1 molecule (*12*).

In our previous studies, the introduction of a strongly hydrophilic lysine to replace the original, more hydrophobic, amino acids between residues 604−610 drastically reduced the apparent affinity of the SGLT1 to phlorizin. According to Hirayama's (*11*) electrophysiological studies using a human Na^+/glucose cotransporter expressed in Xenopus oocytes, the aglucone, which is coplanar with the pyranose ring, should be binding to a hydrophobic/aromatic surface of at least 7 × 12 Å, and mainly through hydrophobic interaction which may occur at several positions. Here, we not only showed that the loop 13 can interact with phlorizin but also demonstrated that replacing the hydrophobic amino acids in position 606 and 609 decreased phlorizin affinity of loop 13, confirming that this hydrophobic region of loop 13 is indeed involved in phlorizin binding. Our previous studies also showed that in transfected COS-7 cells the α-methyl D-glucose uptake affinity was not affected as much as phlorizin inhibition when replacing the hydrophobic amino acids with Lys, indicating that the hydrophobic region may not be responsible for the glucose binding. In the current investigation, we found that high concentrations of D-glucose did not change the fluorescence of loop 13. Although binding not always elicits fluorescence changes, we would rather take this finding as evidence that loop 13 does not interact with the sugar and thus is not involved directly in glucose binding by SGLT1. Our data also demonstrated that phloretin can bind to loop 13 with almost the same affinity as that of phlorizin, which is the direct evidence of aglucone interaction with loop 13. According to Oulianova's (*10*) studies, the phlorizin dissociation constant during the formation of the initial collision complex is 12−30 μM, which is in good agreement to our phlorizin binding K_d value. All these results further support the assumption that loop 13 is involved in aglucone binding through hydrophobic interactions. Changes in the binding affinity of loop 13 appear, however, also to affect the second step of phlorizin binding which is stabilized by Na^+ and probably involves the D-glucose binding site of SGLT1. This could explain why the differences in phlorizin affinity between the wild type and the mutants observed in the current studies are smaller than in the studies on the complete SGLT1 in the intact cells. Such interaction could also be concluded from molecular recognition atomic force experiments where D-glucose affected the conformation of loop 13 in the intact membrane (*14*).

Wielert-Badt et al. (*15*) used 2D-NMR to probe the conformation of the phlorizin. Their modeling indicated that hydrogen bonds from the 2-, 3-, 4-, and 6-hydroxyl group of the pyranoside ring and from the 4′- and 6′-OH groups of the aromatic ring A are important for phlorizin binding. It has been shown that the 3-iodoacetamido-phlorizin bound to an atomic force microscopy cantilever interacts with SGLT1 in a sodium-dependent manner in intact membrane vesicles (*16*). Since the iodoacetamido group is located at the aromatic ring B of the aglucone, it is reasonable to assume that also under these conditions the aromatic ring A of the aglucone interacted with loop 13.

With regard to the disulfide bond of recombinant loop 13 which is very important for phlorizin-dependent tryptophan fluorescence quenching, it should place Trp 561 which is just adjacent to Cys 560 close to Cys 608. Cys 608 is very important for phlorizin binding and was suggested to be located in the site that is involved in phlorizin binding (*12*). The obvious different fluorescence intensity at an excitation lower than 295 nm between wild-type loop 13 and mutant Y604K (replacement Tyr 604 with Lys) indicates that Trp 561 is also close to Tyr 604 (Figure 6). Therefore, it suggests that Trp 561 is close to the region (amino acids 604−610) that is important for phlorizin binding. The fluorescence intensity around 280 nm of loop 13 treated with 2-ME was obviously lower than that of wild-type loop 13. The decreased FRET between Tyr 604 and Trp 561 in the

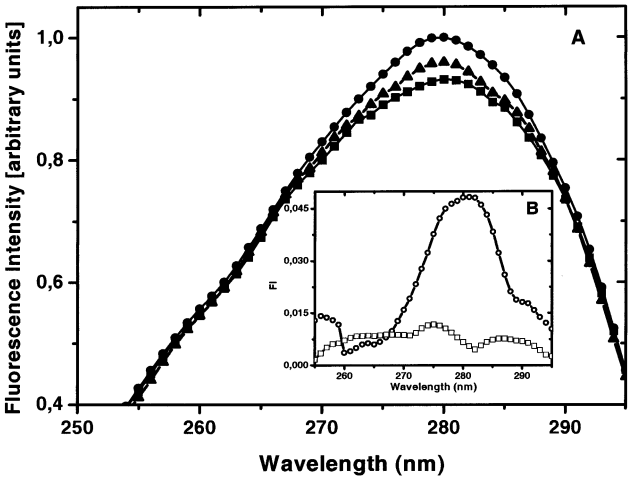

FIGURE 6: (A) Fluorescence excitation spectra of wild type loop 13 (in the absence or presence of 2-ME) and mutant Y604K. (B) Difference fluorescence excitation spectra between loop 13 treated and untreated with 2-ME. Emission spectra were recorded at 350 nm, where Trp 561 contributes exclusively. Final excitation spectra are normalized to equal intensity at 295 nm, where only Trp is excited and no energy transfer occurs. Then the difference fluorescence intensity should be correspond to the energy transfer between Try and Trp. The excitation spectra include: wild-type loop 13 (●), wild-type loop 13 treated with 2-ME (▲), mutant Y604K (■). The difference excitation spectra include: wild-type loop 13 (○), Y604K (□).

presence of excess 2-ME means that the distance between Tyr 604 and Trp 561 becomes large when the disulfide bond is broken down. This indicates the conformational changes of loop 13 upon reducing the disulfide bond, and then no obvious phlorizin-dependent fluorescence quenching could be observed.

It had been observed that treatment of brush border membrane with dithiothreitol reduced phlorizin binding (*15*). The lack of phlorizin-induced fluorescence changes of loop 13 in the presence of 2-ME may be interpreted to support the view that the disulfide bond between Cys 560 and Cys 608 is important for phlorizin binding. However, this effect could also be due to a positional rearrangement that changes the vicinity between Trp 561 and the important amino acids involved in phlorizin binding. Recent mutagenesis data (unpublished results) showed that replacement of Cys 560 with Ala did not alter the phlorizin inhibition of SGLT1 mediated α-methyl D-glucose uptake. Therefore, it is possible that the function of the disulfide bond in recombinant loop 13 is to put Trp 561 close to the amino acids 604−610, thereby facilitating the phlorizin-dependent tryptophan fluorescence quenching via conformational changes. Additional studies are necessary to provide further information on the conformation and dimensions of the phlorizin binding site, as well as the role of SH-groups in phlorizin binding.

ACKNOWLEDGMENT

The careful secretarial work of Natascha Kist is gratefully acknowledged.

REFERENCES

1. Hirayama, B. A., Loo, D. D., and Wright, E. M. (1997) *J. Biol. Chem. 272*, 2110−2115.
2. Loo, D. D., Hirayama, B. A., Gallardo, E. M., Lam, J. T., Turk, E., and Wright, E. M. (1998) *Proc. Natl. Acad. Sci. U.S.A. 95*, 7789−7794.
3. Veenstra, M., Turk, E., and Wright, E. M. (2002) *J. Membr. Biol. 185*, 249−255.
4. Vayro, S., Lo, B., and Silverman, M. (1998) *Biochem. J. 332 (Pt 1)*, 119−125.
5. Panayotova-Heiermann, M., Eskandari, S., Turk, E., Zampighi, G. A., and Wright, E. M. (1997) *J. Biol. Chem. 272*, 20324−20327.
6. Lo, B., and Silverman, M. (1998) *J. Biol. Chem. 273*, 29341−29351.
7. Diez-Sampedro, A., Wright, E. M., and Hirayama, B. A. (2001) *J. Biol. Chem. 276*, 49188−49194.
8. Diedrich, D. F. (1966) *Arch. Biochem. Biophys. 117*, 248−256.
9. Oulianova, N., Falk, S., and Berteloot, A. (2001) *J. Membr. Biol. 179*, 223−242.
10. Oulianova, N., and Berteloot, A. (1996) *J. Membr. Biol. 153*, 181−194.
11. Hirayama, B. A., Diez-Sampedro, A., and Wright, E. M. (2001) *Br. J. Pharmacol. 134*, 484−495.
12. Novakova, R., Homerova, D., Kinne, R. K., Kinne-Saffran, E., and Lin, J. T. (2001) *J. Membr. Biol. 184*, 55−60.
13. Lakowicz, J. R. (1999) *Principles of Fluorescence Spectroscopy*, Kluwer Academic/Plenum, New York.
14. Wielert-Badt, S., Hinterdorfer, P., Gruber, H. J., Lin, J. T., Badt, D., Wimmer, B., Schindler, H., and Kinne, R. K. (2002) *Biophys. J. 82*, 2767−2774.
15. Wielert-Badt, S., Lin, J. T., Lorenz, M., Fritz, S., and Kinne, R. K. (2000) *J. Med. Chem. 43*, 1692−1698.
16. Turner, R. J., and George, J. N. (1984) *Biochim. Biophys. Acta 769*, 23−32.

BI020695B